Observer-based Adaptive Fuzzy Backstepping Tracking Control of Quadrotor Unmanned Aerial Vehicle Powered by Li-ion Battery

Fouad Yacef, Omar Bouhali, Mustapha Hamerlain, Nassim Rizoug

Observer-based Adaptive Fuzzy Backstepping Tracking Control of Quadrotor Unmanned Aerial Vehicle Powered by Li-ion Battery

Article *in* Journal of Intelligent & Robotic Systems · December 2016

DOI: 10.1007/s10846-016-0345-0

CITATIONS
61

READS
500

4 authors, including:

Yacef Fouad
Centre Algérien de Développement des Technologies Avancées
38 PUBLICATIONS **396** CITATIONS

SEE PROFILE

Omar Bouhali
University of Jijel
74 PUBLICATIONS **853** CITATIONS

SEE PROFILE

Mustapha Hamerlain
Centre de Développement des Technologies Avancées, EMP
124 PUBLICATIONS **979** CITATIONS

SEE PROFILE

J Intell Robot Syst (2016) 84:179–197
DOI 10.1007/s10846-016-0345-0

Observer-based Adaptive Fuzzy Backstepping Tracking Control of Quadrotor Unmanned Aerial Vehicle Powered by Li-ion Battery

Fouad Yacef · Omar Bouhali · Mustapha Hamerlain · Nassim Rizoug

Received: 15 December 2014 / Accepted: 27 January 2016 / Published online: 12 February 2016

Abstract In this paper, an Adaptive Fuzzy Backstepping Control (AFBC) approach with state observer is developed. This approach is used to overcome the problem of trajectory tracking for a Quadrotor Unmanned Aerial Vehicle (QUAV) under wind gust conditions and parametric uncertainties. An adaptive fuzzy controller is directly used to approximate an unknown nonlinear backstepping controller which is based on the exact model of the QUAV. Besides, a state observer is constructed to estimate the states. The stability analysis of the whole system is proved using Lyapunov direct method. Uniformly Ultimately Bounded (UUB) stability of all signals in the closed-loop system is ensured. The proposed control method guarantees the tracking of a desired trajectory, attenuates the effect of external disturbances such as wind gust, and solves the problem of unavailable states for measurement. Extended simulation studies are presented to highlight the efficiency of the proposed AFBC scheme.

Keywords Adaptive fuzzy control · Backstepping design · Quadrotor · State observer · Trajectory tracking

F. Yacef (✉) · M. Hamerlain
Division Productique et Robotique, Centre de Développement des Technologies Avancées (CDTA), Algiers, Algeria
e-mail: fyacef@cdta.dz

F. Yacef · O. Bouhali
Laboratoire MécaTronique (LMT), Université de Jijel, Jijel, Algeria

N. Rizoug
Ecole Supérieure des Techniques Aéronautiques et de Construction Automobile (ESTACA), Laval, France

1 Introduction

Unmanned Aerial Vehicles (UAVs) is an attractive area for both civilian and military applications. Due to the wide range application of rotary wings UAVs, it becomes an interesting field that has motivated the control community. Because of its high maneuverability and simple mechanical structure, the QUAV has become a benchmark research platform. However, the control design for this type of vehicles is a complicated step since they are underactuated mechanical systems [1]. The design of a controller for these aircraft needs some important considerations to be taken into account. These kinds of UAVs have a high nonlinear and time-varying behavior, parametric uncertainties and are affected by atmospheric turbulence. Therefore, a robust adaptive control strategy is required to achieve accurate tracking and high performances in an autonomous flight with disturbance rejection capabilities [2]. In addition there are various sources of uncertainties in the QUAV system;

for example, actuator failure, aerodynamic disturbances, and uncertain time delays in the communication system [3].

Many studies have been made to control the QUAV. The first solutions were proposed to overcome the fully-actuated attitude control problem. In [4] a quaternion based PD^2 controller for exponential attitude stabilization was proposed. The authors in [5] designed a control algorithm based on Lyapunov analysis for quadrotor stabilization. A classical approach (PID) and a modern technique (LQ) were applied to the quadrotor attitude control in [6]. The underactuated trajectory tracking problem was handled using backstepping [7, 8] and sliding mode control techniques [9, 10]. In [11] the authors gave a solution to the time scale separation assumption by means of a tracking differentiator and used a new command-filtered compensation for quadrotor trajectory control. Nested saturation algorithm combined with backstepping and feedback control technique has been used for the QUAV [12, 13] and for underactuated systems [14–16], by considering bounds of control inputs nested saturation technique can provide uncoupled and explicitly-given inputs [17]. In view of external disturbances, unknown dynamics and parameter uncertainties, robust backstepping and adaptive control techniques were widely employed. Madani and Benallegue [18] proposed a sliding mode observer to estimate the effect of external disturbances in order to compensate for them. The global closed-loop system composed of backstepping controller and sliding mode observer is robust, but very conservative when the disturbance upper-bound cannot be exactly obtained. Pollini and Metrangolo [19] proposed a robust backstepping controller based on the idea of practical stability to deal with measurement disturbances and actuator failure. Based on sliding mode and adaptive control techniques, a trajectory control of a quadrotor was proposed in [20] to deal with slow and fast time-varying wind conditions. Ramirez-Rodriguez [21] designed a robust backstepping controller based on integral sliding mode for underactuated dynamic model of a quadrotor subject to smooth bounded disturbances. The authors in [22] proposed a nonlinear adaptive tracking controller based on backstepping techniques that can estimate and compensate the effect of mass uncertainty. In [23] a projection-based adaptive control scheme was designed to estimate the unknown parameters, where a state feedback control system and an integrator backstepping approach was used for tracking control of an underactuated quadrotor. In [24] a model predictive control strategy for quadrotor trajectory tracking was proposed, robustness against atmospheric disturbances and optimal control actions were ensured, but the stability proof of the closed-loop system was not given.

In the last decade, backstepping control technique has been an intuitive solution to the underactuated problem for QUAV control. Through slaving the actuated subsystem (attitude) and providing a virtual controller, it can stabilize the underactuation subsystem (position). Unfortunately, this systematic approach requires full knowledge of the system's dynamic which is an extremely difficult assumption to have in practice for UAVs [21]. To undertake this problem and extend the applicability of backstepping, different schemes have been proposed by combining backstepping with other techniques, such as function approximation using neural network [25]. In [26] the authors used two neural networks to estimate aerodynamic forces and moments. Backstepping approach and Lagrange form dynamics were used for quadrotor controller design. Where in [27] a neural network observer was proposed to attenuate the measurement noise. Nevertheless, these schemes resulted in a complicated algorithms that adds additional complexity to the classical backstepping algorithm.

Fuzzy Logic Systems (FLSs) were known as a powerful approximators [28]. They have been extensively used for modeling and controlling of uncertain nonlinear systems, due to their universal approximation properties. Over the past few years, various adaptive fuzzy control approaches have been developed for different classes of nonlinear systems [29–38]. In [39–41], adaptive fuzzy control schemes based on backstepping approach have been developed for uncertain nonlinear systems, where the stability of the resulting closed-loop systems were gained using the well-known Lyapunov direct method. In this work, we propose to use this powerful approximation technique to compensate for unknown dynamics and uncertainties in the QUAV system. The control algorithms mentioned previously [11, 21] and [22] suffer from their requirements to measure directly the state variables. In practice, the use of sensors to measure the quadrotor attitude and position increases the cost and the complexity of the system. That is why, a state

observer is an attractive solution to estimate the QUAV states.

Motivated by the previous discussion, in this paper, the problem of position control is investigated for an underactuated QUAV subject to aerodynamic disturbances such as wind gust and parametric uncertainties via fuzzy-approximation-based adaptive control. A FLS with the aid of adaptive estimators to approximate unknown nonlinear dynamics, as well as a robust adaptive compensation to attenuate the effect of external disturbances and compensate approximation errors are employed. The present paper provides further results on the QUAV trajectory control accounting for state estimation, wind gust effect attenuation, and the use of σ-modification term in the adaptive law which were ignored in the control design in [42]. The main contributions of this paper are : (i) the proposal of an AFBC scheme for quadrotor trajectory tracking with robustness against uncertainties and attenuation of wind gust disturbances; (ii) no dependency on the mathematical model by combining FLS with backstepping; and (iii) UUB stability of the global controller/observer closed-loop system.

The remaining of this paper is organized as follows: In Section 2, the dynamic model of the QUAV and the wind gust model are presented. Then, in Section 3, problem formulation and some preliminaries are presented. The proposed control approach and the stability proof of the closed-loop system are illustrated in Section 4. Some simulation results are depicted to show the effectiveness of the proposed controller in Section 5. Finally, some conclusions are drawn in Section 6.

2 Quadrotor Modeling

Different models have been proposed in literature for the QUAV. The authors in [43, 44] and [17] considered the quadrotor as a rigid body, and used the Euler-Lagrange formulation with small angles approximation to derive a simplified model for described the quadrotor dynamics. In [18] A nonlinear full model was derived using the Newton-Euler approach, the aerodynamic moments and forces effects are considered. In [6] a simplified model of the quadrotor is proposed including rigid body dynamics, gyroscopic effect, and aerodynamic forces. Finally, [45, 46] focus on the modeling of aerodynamic effects and blade flapping for the quadrotor.

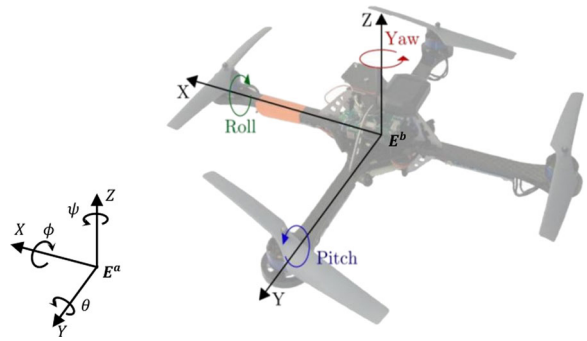

Fig. 1 Quadrotor scheme

The QUAV shown in Fig. 1, has four rotors to generate the propeller forces. Its configuration simplifies the displacement and increases the lift force. On varying the rotor speeds altogether with the same quantity, the lift forces will change, affecting in this case the altitude of the vehicle. One pair of rotors turn in clockwise direction while the second pair turn in the opposite direction in order to balance the moments and produce yaw motion as needed. Yaw angle is obtained by speeding up or slowing down the clockwise motors. The horizontal motion depends on the pitch and roll angles.

2.1 Quadrotor Dynamics

Two frames are used to study the system motion: a frame integral with the earth $E^a(O^a, e_1^a, e_2^a, e_3^a)$ which is supposed to be inertial, and a body-fixed frame $E^b(O^b, e_1^b, e_2^b, e_3^b)$ where O^b is fixed to the center of mass of the quadrotor. The absolute position of the quadrotor is described by $\xi = [x, y, z]^T$ and its attitude by the Euler angles $\eta = [\phi, \theta, \psi]^T$. The attitude angles are respectively Yaw angle (ψ rotation around z-axis), Pitch angle (θ rotation around y-axis) and Roll angle (ϕ rotation around x-axis), see Fig. 1. Let $V = [u, v, w]^T \in E^b$ denote the linear velocity and $\Omega = [p, q, r]^T \in E^b$ denote the angular velocity of the airframe expressed in the body-fixed-frame. The relation between the velocities vectors (V, Ω) and (ξ, η) is [18]:

$$\begin{aligned} \dot{\xi} &= R(\eta)V \\ \Omega &= N(\eta)\dot{\eta} \end{aligned} \tag{1}$$

where $R(\eta)$ and $N(\eta)$ are respectively the transformation velocity matrix and the rotation velocity matrix between E^a and E^b, such as:

$$R(\eta) = \begin{bmatrix} C_\theta C_\psi & S_\phi S_\theta C_\psi - C_\phi S_\psi & C_\phi S_\theta C_\psi + S_\phi S_\psi \\ C_\theta S_\psi & S_\phi S_\theta S_\psi + C_\phi C_\psi & C_\phi S_\theta S_\psi - S_\phi C_\psi \\ -S_\theta & S_\phi C_\theta & C_\phi C_\theta \end{bmatrix}$$

$$N(\eta) = \begin{bmatrix} 1 & 0 & -S_\theta \\ 0 & C_\phi & C_\theta S_\phi \\ 0 & -S_\phi & C_\theta C_\phi \end{bmatrix}$$

The derivation of (1) with respect to time gives

$$\begin{aligned} \ddot{\xi} &= R(V + \dot{\Omega} \times V) \\ \dot{\Omega} &= N\ddot{\eta} + (\frac{\partial N}{\partial \phi}\dot{\phi} + \frac{\partial N}{\partial \theta}\dot{\theta})\dot{\eta} \end{aligned} \tag{2}$$

Using the Newton's laws in the body-fixed frame E^b, about the QUAV subjected to forces $\sum F_{ext}$ and moments $\sum T_{ext}$ applied to the center of mass, one obtains the dynamic equation motions [18]:

$$\begin{aligned} \ddot{\xi} &= \frac{1}{m} R \sum F_{ext} \\ \ddot{\eta} &= (IN)^{-1}[\sum T_{ext} - I(\frac{\partial N}{\partial \phi}\dot{\phi} + \frac{\partial N}{\partial \theta}\dot{\theta})\dot{\eta} \\ &\quad -(N\dot{\eta}) \times (IN\dot{\eta})] \end{aligned} \tag{3}$$

with $\sum F_{ext}$ and $\sum T_{ext}$ include the external forces/torques applied in the center of mass of the QUAV according to the direction of the body-fixed frame E^b, such as:

$$\begin{aligned} \sum F_{ext} &= F + F_{grav} \\ \sum T_{ext} &= T + T_{gyro} \end{aligned} \tag{4}$$

where F and T are the forces and torques produced by the propeller system, respectively. F_{grav} is the gravity effect force with $G = [0, 0, g]^T$ the gravity vector, and T_{gyro} define the gyroscopic effects resulting from the propeller rotations. These variables are defined as:

$$F = \begin{bmatrix} 0 \\ 0 \\ b\sum_{i=1}^{4} \omega_i^2 \end{bmatrix}, T = \begin{bmatrix} lb(\omega_3^2 - \omega_1^2) \\ lb(\omega_4^2 - \omega_2^2) \\ d\sum_{j=1}^{4}(-1)^{i+1}\omega_i^2 \end{bmatrix},$$

$$\begin{aligned} F_{grav} &= mR(\eta)^T G \\ T_{gyro} &= -\sum_{j=1}^{4} \Omega \times I_r(-1)^{i+1}\omega_i \end{aligned}$$

where l is de distance between the rotor shaft and the center of mass, d is the drag factor, b is the thrust factor and I_r is the rotor inertia.

The quadrotor mathematical model (3), can be expressed in a state space form as:

$$\dot{X} = f(X, U) + W \tag{5}$$

with the following state vector $X = [x_{11}, x_{21}, \ldots, x_{16}, x_{26}]^T \in \Re^{12}$, input vector $U = [u_1, u_2, u_3, u_4]^T$ and $W = [0, w_{g1}, \ldots, 0, w_{g6}]^T \in \Re^{12}$ is the effect of external disturbances that affect the movement of the QUAV and are produced by unknown wind gust.

$$\begin{aligned} &x_{11} = \phi, x_{22} = \dot{\theta}, x_{14} = z, x_{25} = \dot{x} \\ &x_{21} = \dot{\phi}, x_{13} = \psi, x_{24} = \dot{z}, x_{16} = y \\ &x_{12} = \theta, x_{23} = \dot{\psi}, x_{15} = x, x_{26} = \dot{y} \end{aligned}$$

$$\begin{aligned} u_1 &= F_3 - F_1 \\ u_2 &= F_4 - F_2 \\ u_3 &= F_1 - F_2 + F_3 - F_4 \\ u_4 &= F_1 + F_2 + F_3 + F_4 \\ \omega &= \omega_1 - \omega_2 + \omega_3 - \omega_4 \end{aligned} \tag{6}$$

where $F_j = b\omega_j^2$ $(j = 1, \ldots, 4)$ is the force generated by the j-th rotor. The nonlinear function $f(X, U)$ is given by:

$$f(X,U) = \begin{pmatrix} x_{21} \\ x_{22}x_{23}a_1 + x_{22}a_2\omega + b_1u_1 \\ x_{22} \\ x_{21}x_{23}a_3 + x_{21}a_4\omega + b_2u_2 \\ x_{23} \\ x_{21}x_{22}a_5 + b_3u_3 \\ x_{24} \\ -g + \frac{C_{x_{11}}C_{x_{12}}}{m}u_4 \\ x_{25} \\ \frac{u_4}{m}(C_{x_{11}}S_{x_{12}}C_{x_{13}} + S_{x_{11}}S_{x_{13}}) \\ x_{26} \\ \frac{u_4}{m}(C_{x_{11}}S_{x_{12}}S_{x_{13}} - S_{x_{11}}C_{x_{13}}) \end{pmatrix} \tag{7}$$

with $C_{(.)}$ and $S_{(.)}$ represent $cos(.)$ and $sin(.)$ respectively and

$$\begin{aligned} a_1 &= \frac{I_y - I_z}{I_x}, \; a_4 = \frac{-I_r}{I_y}, \quad b_2 = \frac{l}{I_y} \\ a_2 &= \frac{I_r}{I_x}, \quad a_5 = \frac{I_x - I_y}{I_z}, \; b_3 = \frac{d}{bI_z} \\ a_3 &= \frac{I_z - I_x}{I_y}, \; b_1 = \frac{l}{I_x} \end{aligned}$$

2.2 Battery Model

The QUAV is typically supplied by Lithium ion batteries, because of their high energy density, high charge and discharge rates, long lifetime, lack of memory effect [47] and affordable cost. In this study a Li-ion battery model [48] was used in order to analyze the power consumed by the QUAV and estimate time flight. The used battery model have 6 parallel branch and 1 series branch, with $3.6volt$ for each branch which mean that the battery have $21.6volt$ and a capacity of $1.55Ah$.

First we calculate the power provided by the QUAV, $P = \sum_{j=1}^{4} \tau_j \omega_j$, where τ_j is the torque generated by the j-th rotor. Then we calculate the current, $I_{bat} = \frac{P}{\kappa V_{bat}}$ where $\kappa = 0.8$ is the energy efficiency coefficient. The battery current, I_{bat} is the input of battery model where the voltage V_{bat} and the state of charge SOC are the outputs.

2.3 Wind Gust Model

Wind gust is a complex physical phenomenon. It is typically modeled using deterministic model [49] or stochastic model [50]. The second model assumes that the turbulence is a stationary Gaussian random process, which is the most common assumption. The stationary characteristic implies that the turbulence is infinite in duration, while the idea of a Gaussian process is related to the probability of obtaining a given gust velocity at a specific time.

The Power Spectral Density (PSD) is a stochastic approach. In the PSD atmospheric turbulence model, it is assumed that the intensity of the turbulence depends significantly on specific circumstances and is subject to changes owing to weather conditions, flight altitude, and temperature gradient [51].

The wind gust signal is generated by passing a white noise through a forming filter. In literature, two main forming filters can be found: the Dryden and the Von Karman filter. As the Dryden filter has a simpler form than the Von Karman's we prefer to use it in this work. The filters used to generate the Dryden spectral model are given by [52]:

$$H_u(s) = \frac{\Delta u}{N_W} = \sigma_u \sqrt{\frac{2L_u}{\pi v}} \frac{1}{1 + \frac{L_u}{v}s} \tag{8}$$

$$H_v(s) = \frac{\Delta v}{N_W} = \sigma_v \sqrt{\frac{L_v}{\pi v}} \frac{1 + \frac{\sqrt{3}L_v}{v}s}{(1 + \frac{L_v}{v}s)^2} \tag{9}$$

$$H_w(s) = \frac{\Delta w}{N_W} = \sigma_w \sqrt{\frac{L_w}{\pi v}} \frac{1 + \frac{\sqrt{3}L_w}{v}s}{(1 + \frac{L_w}{v}s)^2} \tag{10}$$

where N_W is a white noise, v denotes the relative speed of the QUAV to air stream and $[\Delta u, \Delta v, \Delta w]^T$ is the change in body linear velocities due to wind gust. The turbulence intensities $(\sigma_u, \sigma_v, \sigma_w)$ and the turbulence scale lengths (L_u, L_v, L_w) describe the behavior of the wind gust. In low altitude region (altitude < 1000 ft), turbulence scale length and intensities are given by:

$$L_w = h, L_u = L_v = \frac{h}{(0.177 + 0.000823h)^{1.2}} \tag{11}$$

$$\sigma_w = 0.1W_{20}, \frac{\sigma_u}{\sigma_w} = \frac{\sigma_v}{\sigma_w} = \frac{1}{(0.177 + 0.000823h)^{0.4}} \tag{12}$$

where h is the height above ground and W_{20} is the wind speed expressed in Beaufort Scale (BS). In this paper, we have considered a typical wind speed of $3.4m/s$ (BS 3) and an altitude of $3m$.

2.4 Virtual Control

The dynamic model (5) of the quadrotor has six outputs $(x, y, z, \phi, \theta, \psi)$ while it has only four independent inputs (u_1, u_2, u_3, u_4). Therefore, the quadrotor is an underactuated system. We are not able to control all of the states at the same time [18]. A possible combination of controlled outputs can be (x, y, z, ψ) in order to track the desired positions and stabilize roll and pitch angle (ϕ, θ) which introduces stable zero dynamics into the system. To deal with this problem, we need to create two virtual control inputs (u_5, u_6) in addition to four control inputs of the quadrotor, so that every output of the system will be controlled independently. The virtual control inputs u_5 and u_6 represent the relation between pitch and x motion; roll and y motion respectively [42].

$$u_5 = \frac{u_4}{m}(C_{x_{11}} S_{x_{12}} C_{x_{13}} + S_{x_{11}} S_{x_{13}}) \tag{13}$$

$$u_6 = \frac{u_4}{m}(C_{x_{11}} S_{x_{12}} S_{x_{13}} - S_{x_{11}} C_{x_{13}}) \tag{14}$$

with $C_{(.)}$ and $S_{(.)}$ represent $cos(.)$ and $sin(.)$ respectively. Using the approximation of the control law u_4

$$u_4 = \frac{mg}{C_{x_{11}} C_{x_{12}}} \tag{15}$$

Substituting (15) in (13) and (14), and by $C_{x_{13}}(13) + S_{x_{13}}(14)$ we have

$$\left(\frac{u_5 C_{x_{13}} + u_6 S_{x_{13}}}{g}\right) = tan(x_{12}) \tag{16}$$

Applying $S_{x_{13}}(13) - C_{x_{13}}(14)$ one have

$$\left(\frac{u_5 S_{x_{13}} - u_6 C_{x_{13}}}{g} C_{x_{12}}\right) = tan(x_{11}) \tag{17}$$

From (16) and (17), with $x_{11} = \phi_d, x_{12} = \theta_d, x_{13} = \psi$ we obtain

$$\begin{aligned} \theta_d &= atan\left(\frac{u_5 \cos\psi + u_6 \sin\psi}{g}\right) \\ \phi_d &= atan\left(\frac{u_5 \sin\psi - u_6 \cos\psi}{g} \cos\theta_d\right) \end{aligned} \tag{18}$$

The physical significance of virtual controls is that the lateral motion (x, y) is controlled by roll and pitch angles. That is the rolling and pitching motions must take desired angles (ϕ_d, θ_d) to guarantee the control tracking of lateral motion. Figure 2 shows the actuated QUAV with six inputs $(u_1, \ldots, u_6)$, and six outputs $(\phi, \theta, \psi, z, x, y)$.

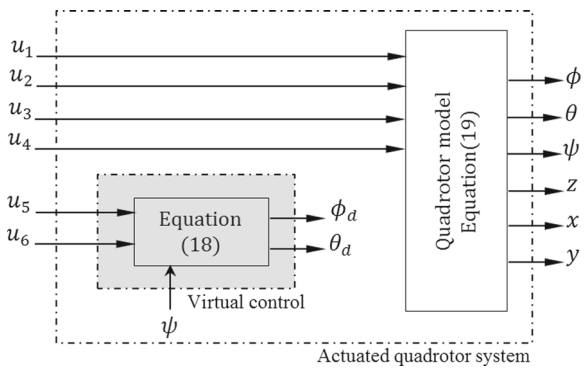

Fig. 2 Actuated QUAV with virtual control

3 Problem Formulation and Preliminaries

3.1 Control Problem Formulation

The main objective of the control design is to develop an observer-based adaptive fuzzy tracking controller able to generate the input signals for quadrotor motors ensuring that the outputs $(x(t), y(t), z(t), \psi(t))$ track asymptotically the desired trajectory $(x_d(t), y_d(t), z_d(t), \psi_d(t))$, while ensuring that all involved signals in the closed-loop system remain bounded.

The state space model (5) can be rearranged as follows:

$$\begin{aligned} \dot{x}_{1i} &= x_{2i} \\ \dot{x}_{2i} &= f_i(X) + g_i(X) u_i(t) + w_i \\ y_i &= x_{1i} \end{aligned} \tag{19}$$

where $i = 1, \ldots, M$, $M = 6$ is the number of subsystem, $f_i(X)$ and $g_i(X)$, are unknown nonlinear smooth functions, $u = [u_1, \ldots, u_6]^T \in \Re^6$ is the control input vector, $Y = [y_1, \ldots, y_6]^T \in \Re^6$ is the output vector and $W = [0, w_1, \ldots, 0, w_6]^T$ is wind gust vector.

$$\begin{aligned} f_1(X) &= x_{22} x_{23} a_1 + x_{22} a_2 \omega,\ g_1(X) = \frac{l}{I_x} \\ f_2(X) &= x_{21} x_{23} a_3 + x_{21} a_4 \omega,\ g_2(X) = \frac{l}{I_y} \\ f_3(X) &= x_{21} x_{22} a_5,\ g_3(X) = \frac{d}{b I_z} \\ f_4(X) &= -g,\ g_4(X) = \frac{C_{x_{11}} C_{x_{12}}}{m} \\ f_5(X) &= 0,\ g_5(X) = 1 \\ f_6(X) &= 0,\ g_6(X) = 1 \end{aligned}$$

The following assumptions are considered:

Assumption 1 The desired trajectory $x_{1i,d}$ is a smooth function of t, and $x_{1i,d}$, $\dot{x}_{1i,d}$, and $\ddot{x}_{1i,d}$ are bounded.

Assumption 2 The control inputs $F_j (j = 1, ..., 4)$ are bounded.

Assumption 3 The yaw, pitch and roll angels are limited to $(-\pi \leq \psi \leq \pi)$, $(-\frac{\pi}{2} \leq \theta \leq \frac{\pi}{2})$ and $(-\frac{\pi}{2} \leq \phi \leq \frac{\pi}{2})$.

Assumption 4 The functions $g_i(X)$ are positive definite, slowly varying and bounded.

Let's define the tracking error variable for the reference signal $x_{1i,d}$ as:

$$z_{1i} = x_{1i,d} - x_{1i}, i = 1, \ldots, 6$$

Step 1. From the first differential equation of (19), the dynamic of first error is given by $\dot{z}_{1i} = \dot{x}_{1i,d} - x_{2i}$. Now, let choose the Lyapunov function candidate as $V_{1i} = \frac{1}{2} z_{1i}^2$, and its time derivative $\dot{V}_{1i}$ as follows:

$$\dot{V}_{1i} = z_{1i}\dot{z}_{1i} = z_{1i}(\dot{x}_{1i,d} - x_{2i}) \tag{20}$$

We construct the virtual control law α_i as

$$\alpha_i = \dot{x}_{1i,d} + c_{1i} z_{1i} \tag{21}$$

where c_{1i} is a design parameter, and $z_{2i} = \alpha_i - x_{2i}$. By using (21), the time derivative of V_{1i} (20) can be rewritten in the following form:

$$\dot{V}_{1i} = -c_{1i} z_{1i}^2 + z_{1i} z_{2i} \tag{22}$$

Step 2. Differentiating z_{2i} and using (19) gives

$$\dot{z}_{2i} = \dot{\alpha}_i - f_i(X) - g_i(X) u_i(t) - w_i \tag{23}$$

Choose the augmented Lyapunov function candidate as $V_{2i} = V_{1i} + \frac{1}{2g_i(X)} z_{2i}^2$. Then, the time derivative of V_{2i} will be

$$\dot{V}_{2i} = \dot{V}_{1i} + \frac{1}{g_i(X)} z_{2i}\dot{z}_{2i} - \frac{\dot{g}_i(X)}{2g_i^2(X)} z_{2i}^2 \tag{24}$$

By substituting (22) and (23) into (24), one obtains

$$\dot{V}_{2i} = -c_{1i} z_{1i}^2 + z_{2i}\left[\frac{\dot{\alpha}_i + g_i(X) z_{1i} - f_i(X) - w_i}{g_i(X)} - \frac{\dot{g}_i(X)}{2g_i^2(X)} z_{2i} - u_i(t)\right] \tag{25}$$

The control law $u_i(t)$ is designed as

$$u_i(t) = \frac{1}{g_i(X)}[\dot{\alpha}_i + g_i(X) z_{1i} - f_i(X) - w_i - \frac{\dot{g}_i(X)}{2g_i(X)} z_{2i}] + c_{2i} z_{2i} \tag{26}$$

with $\dot{\alpha}_i = \ddot{x}_{1i,d} + c_{1i}(\dot{x}_{1i,d} - \dot{x}_{1i})$. Using (26), it can be easily verified that

$$\dot{V}_{2i} \le -c_{1i} z_{1i}^2 - c_{2i} z_{2i}^2 \tag{27}$$

Assume that $w_i = 0$. The obtained output-feedback controller can be written in the following form

$$u_i(t) = u_{b,i}(t) + c_{2i} z_{2i} \tag{28}$$

$$u_{b,i}(t) = \frac{1}{g_i(X)}[\dot{\alpha}_i + g_i(X) z_{1i} - f_i(X) - \frac{\dot{g}_i(X)}{2g_i(X)} z_{2i}] \tag{29}$$

with $\dot{\alpha}_i = \ddot{x}_{1i,d} + c_{1i}(\dot{x}_{1i,d} - \dot{x}_{1i})$ and $z_{2i} = \alpha_i - x_{2i}$.

Remark 1 Since $\dot{V}_{2i}(t)$ is negative semi-definite, that is $V_{2i}(t) \le V_{2i}(0)$. Therefore, z_{1i} and z_{2i} are uniformly bounded. This implies the boundedness of the closed-loop signals $\dot{z}_{1i}$, $\dot{z}_{2i}$ and $u_i(t)$. Since $V_{2i}(0)$ is bounded, and V_{2i} is non-increasing and bounded from below, the $\lim_{t\to\infty} V_{2i}(t) = V_{2i}(\infty)$ exists. By employing Barbalat's Lemma [53], one can conclude that $z_{1i} \to 0$ and $z_{2i} \to 0$ as $t \to \infty$, which implies the asymptotic converge of tracking errors to zero.

Remark 2 The six control laws $u_{b,i}(t)$ are easily obtained if the nonlinear functions $f_i(X)$ and $g_i(X)$ are known; however these nonlinear functions are unknown. So six FLSs are used to approximate directly these control laws.

3.2 Fuzzy Logic System

A fuzzy logic system consists of four parts: the knowledge base, the fuzzifier, the fuzzy inference engine, and the defuzzifier. The knowledge base is composed of a collection of fuzzy IF-THEN rules in the following form [29]:

$$R^k : \textbf{IF } x_1 is F_1^k and \ldots x_n is F_n^k, \textbf{ THEN } y is G^k, k = 1, 2, \ldots, N.$$

where $X = [x_1, , x_n]^T \in \Re^n$ and $\overline{Y} \in \Re$ are the input and the output vectors, respectively. $F_l^k (l = 1, \ldots, n)$ and G^i are the fuzzy sets associated with the fuzzy membership functions $\mu_{F_l^k}(x_l)$ and $\mu_{G^k}(\overline{Y})$, respectively. N is the number of rules.

By using the singleton fuzzifier, product inference engine, and center average defuzzification [28], the output of the fuzzy logic system can be expressed as follows:

$$\overline{Y}(X \mid \Theta) = \frac{\sum_{k=1}^N \bar{y}_k \prod_{l=1}^n \mu_{F_l^k}(x_l)}{\sum_{k=1}^N [\prod_{l=1}^n \mu_{F_l^k}(x_l)]} \tag{30}$$

where $\bar{y}_k = \max_{y\in\Re} \mu_{G^k}(y)$. Let

$$\varphi_i(X) = \frac{\prod_{l=1}^n \mu_{F_l^k}(x_l)}{\sum_{k=1}^N [\prod_{l=1}^n \mu_{F_l^k}(x_l)]} \tag{31}$$

Denoting $\varphi(X) = [\varphi_1(X), \varphi_2(X), \ldots, \varphi_N(X)]^T$ as the vector of fuzzy basis functions, and $\Theta^T = [\bar{y}_1, \bar{y}_2, \ldots, \bar{y}_N] = [\Theta_1, \Theta_2, \ldots, \Theta_N]$ the vector of consequent parameters. Then, the FLS can be rewritten as follows:

$$\overline{Y}(X \mid \Theta) = \Theta^T \varphi(X) \tag{32}$$

Lemma 1 [28] *For any given real continuous function* $f(X)$ *on the compact set* $\Omega_f \subset \Re^n$ *and arbitrary* $\varepsilon > 0$ *there exists a FLS such that*

$$\sup_{X \in \Omega_f} \mid f(X) - \Theta^T \varphi(X) \mid \leq \varepsilon$$

We assumed that the quadrotor states (19) are not available for measure. So a state observer should be designed to estimate the states, and the AFBC scheme is constructed based on state observer [40].

Using lemma 1 and the proof given in [28], FLSs are universal approximators, i.e., they can approximate any smooth function on a compact set. Based on the approximation capability of FLSs, we can assume that the control laws $u_{b,i}(t)$ (29) can be approximated as:

$$\hat{u}_{b,i}(X \mid \Theta_i) = \Theta_i^T \varphi_i(X) \tag{33}$$

Let $\hat{X}$ be the estimate of X, one has $\hat{u}_{b,i}(\hat{X} \mid \Theta_i) = \Theta_i^T \varphi_i(\hat{X}))$. According to [29], the optimal parameter vector Θ_i^* is defined as:

$$\Theta_i^* = arg \min_{\Theta_i \in \Omega_\theta} \left\{ \sup_{\hat{X} \in \Omega_x} \mid \hat{u}_{b,i}(\hat{X} \mid \Theta_i) - u_{b,i}(t) \mid \right\} \tag{34}$$

where $\Omega_{\hat{x}}$ and Ω_θ are a compact set for $\hat{X}$ and Θ_i respectively. Also, the minimum fuzzy approximation error ε_i is defined as:

$$\varepsilon_i = u_{b,i}(t) - \hat{u}_{b,i}(\hat{X} \mid \Theta_i^*) \tag{35}$$

In this case the control law $u_{b,i}(t)$ can be rewritten as:

$$\begin{aligned} u_{b,i}(t) &= \hat{u}_{b,i}(\hat{X} \mid \Theta_i^*) + \varepsilon_i \\ &= \Theta_i^{*T} \varphi_i(\hat{X}) + \varepsilon_i \end{aligned} \tag{36}$$

Assume that the minimum fuzzy approximation error ε_i has an upper bound $\bar{\varepsilon}_i > 0$, such that $|\varepsilon_i| \leq \bar{\varepsilon}_i$.

3.3 State Observer Design

The high-gain state observer is designed for (19) as follows:

$$\begin{aligned} \dot{\hat{x}}_{1i} &= \hat{x}_{2i} + k_{1i}(y_i - \hat{x}_{1i}) \\ \dot{\hat{x}}_{2i} &= f_i(\hat{X}) + g_i(\hat{X}) u_i(t) + w_i + k_{2i}(y_i - \hat{x}_{1i}) \\ \hat{y}_i &= \hat{x}_{1i} \end{aligned} \tag{37}$$

Rewriting (37) in the following form

$$\begin{aligned} \dot{\hat{x}}_i &= A_i \hat{x}_i + K_i y_i + B_i + G_i u_i(t) + W_i \\ \hat{y}_i &= C^T \hat{x}_i \end{aligned} \tag{38}$$

where

$$A_i = \begin{bmatrix} -k_{1i} & 1 \\ -k_{2i} & 0 \end{bmatrix}, K_i = \begin{bmatrix} k_{1i} \\ k_{2i} \end{bmatrix}, \hat{x}_i = \begin{bmatrix} \hat{x}_{1i} \\ \hat{x}_{2i} \end{bmatrix}$$
$$B_i = \begin{bmatrix} 0 \\ f_i(\hat{X}) \end{bmatrix}, G_i = \begin{bmatrix} 0 \\ g_i(\hat{X}) \end{bmatrix}, W_i = \begin{bmatrix} 0 \\ w_i \end{bmatrix}, C_i = \begin{bmatrix} 1 \\ 0 \end{bmatrix}$$

The vectors K_i are chosen such that A_i are a strict-Hurwitz matrix. Then, given $Q_i^T = Q_i > 0$, there exists a positive definite matrices $P_i^T = P_i > 0$ such that:

$$A_i^T P_i + P_i A_i = -2Q_i \tag{39}$$

Let $e_i = x_i - \hat{x}_i$ be the observer error; then from (38) and (19), we have the observer dynamic

$$\dot{e}_i = A_i e_i + \delta_i \tag{40}$$

where $x_i = [x_{1i}, x_{2i}]^T$, $\delta_i = [0, \delta_{fi} + \delta_{gi}]^T$, $\delta_{fi} = f_i(X) - f_i(\hat{X})$ and $\delta_{gi} = g_i(X) - g_i(\hat{X})$.

Assumption 5 The nonlinear estimated errors δ_{fi}, δ_{gi} are bounded and have an upper bouned, such that $|\delta_{fi}| \leq \bar{\delta}_{fi}$, $|\delta_{gi}| \leq \bar{\delta}_{gi}$, with $\bar{\delta}_{fi}$ and $\bar{\delta}_{gi}$ being positive constants.

4 Controller Design and Stability Proof

4.1 Adaptive Fuzzy Control Design Based on State Observer

In this section, the observer-based adaptive fuzzy backstepping controller and parameter adaptive laws are to be developed such that all internal signals of the closed-loop system are UUB, and the tracking errors $\hat{z}_{1i} = x_{1i,d} - \hat{x}_{1i}$ are as small as desired, see Figs. 3 and 4.

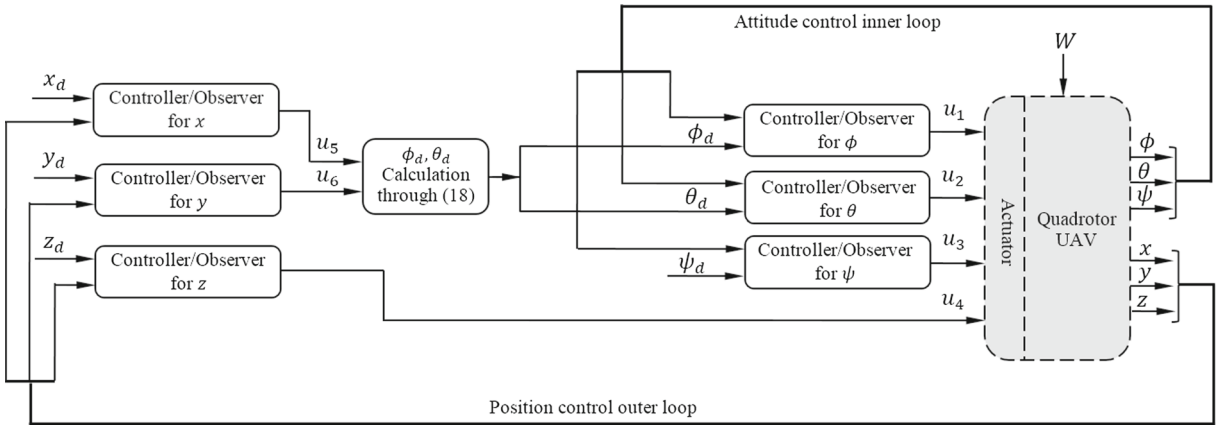

Fig. 3 Quadrotor control scheme

The control inputs system that ensure closed-loop system stability can be determined as:

$$u_i(t) = u_{a,i} + u_{r,i} + u_{p,i}, (i = 1, \ldots, 6) \tag{41}$$

with:

- $u_{a,i} = \hat{u}_{b,i}$ is the fuzzy adaptive control term (42) which is designed to approximate backstepping control law $u_{b,i}(t)$ (29).

$$u_{a,i} = \Theta_i^T \varphi_i(\hat{X}) \tag{42}$$

where $\varphi_i(\hat{X})$ is the vector of fuzzy basis functions, Θ_i is the vector of adjustable parameters of the FLS and is given by:

$$\dot{\Theta}_i = \gamma_i \hat{z}_{2i} \varphi_i(\hat{X}) - \sigma_{1i} \Theta_i \tag{43}$$

where $\gamma_i > 0$ and $\sigma_{1i} > 0$ are design parameters, $\hat{z}_{2i} = \alpha_i - \hat{x}_{2i}$ and $\Theta_i(0) = 0$.

- $u_{r,i}$ is a bounded robust control term employed to compensate the fuzzy approximation error given by:

$$u_{r,i} = \hat{\varepsilon}_i \tanh(\frac{\hat{z}_{2i}}{\epsilon_i}) \tag{44}$$

$$\dot{\hat{\varepsilon}}_i = \eta_i \hat{z}_{2i} \tanh(\frac{\hat{z}_{2i}}{\epsilon_i}) - \sigma_{2i} \hat{\varepsilon}_i \tag{45}$$

where $\eta_i > 0$, $\sigma_{2i} > 0$ and $\epsilon_i > 0$ are design parameters, and $\hat{\varepsilon}_i(0) = 0$.

- $u_{p,i}$ is the proportional derivative term given by:

$$u_{p,i} = c_{2i} \hat{z}_{2i} \tag{46}$$

where $c_{2i} > 0$ are design parameters.

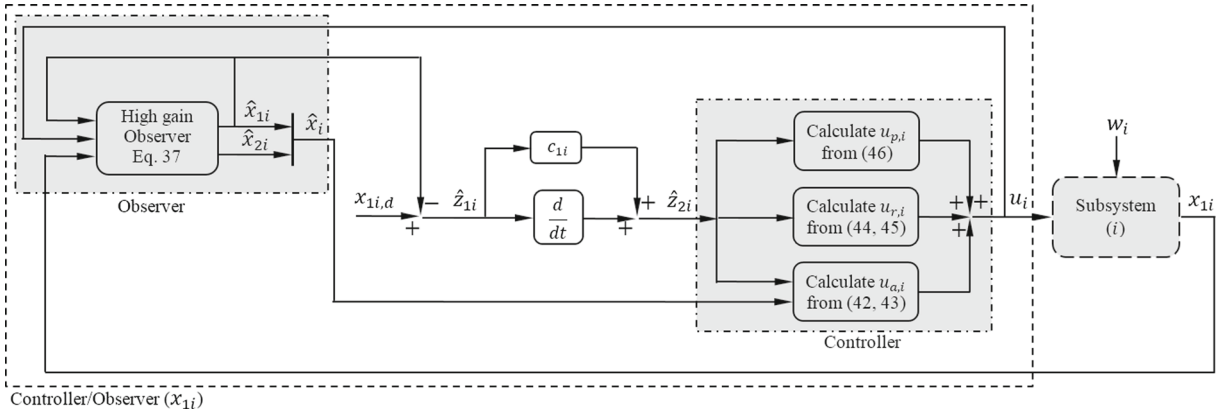

Fig. 4 Observer-based control scheme for i-th sub-system

4.2 Stability Proof

Consider the following Lyapunov function candidate:

$$V = \frac{1}{2}\sum_{i=1}^{6} e_i^T P_i e_i + \hat{z}_{1i}^2 + \frac{1}{g_i(\hat{X})}\hat{z}_{2i}^2 + \frac{1}{\gamma_i}\tilde{\Theta}_i^T\tilde{\Theta}_i + \frac{1}{\eta_i}\tilde{\varepsilon}_i^T\tilde{\varepsilon}_i \tag{47}$$

where $\tilde{\varepsilon}_i = \varepsilon_i^* - \hat{\varepsilon}_i$, $\hat{\varepsilon}_i$ is the estimate of ε_i^* and $\tilde{\Theta}_i = \Theta_i^* - \Theta_i$ is the estimation error.
The time derivative of V along the solution of (40) and using (25) is

$$\begin{aligned}\dot{V} = &\sum_{i=1}^{6} \frac{1}{2}\dot{e}_i^T P_i e_i + \frac{1}{2}e_i^T P_i \dot{e}_i \\ &- c_{1i}\hat{z}_{1i}^2 + \hat{z}_{2i}\left[u_{b,i}(t) - u_i(t)\right] \\ &+ \frac{1}{\gamma_i}\tilde{\Theta}_i^T\dot{\tilde{\Theta}}_i + \frac{1}{\eta_i}\tilde{\varepsilon}_i^T\dot{\tilde{\varepsilon}}_i\end{aligned} \tag{48}$$

$$\begin{aligned}\dot{V} = &\sum_{i=1}^{6} \frac{1}{2}e_i^T[A_i^T P_i + P_i A_i]e_i + e_i^T P_i \delta_i \\ &- c_{1i}\hat{z}_{1i}^2 + \hat{z}_{2i}\left[u_{b,i}(t) - u_i(t)\right] \\ &+ \frac{1}{\gamma_i}\tilde{\Theta}_i^T\dot{\tilde{\Theta}}_i + \frac{1}{\eta_i}\tilde{\varepsilon}_i^T\dot{\tilde{\varepsilon}}_i\end{aligned} \tag{49}$$

$$\begin{aligned}\dot{V} = &\sum_{i=1}^{6} -e_i^T Q_i e_i + e_i^T P_i \delta_i \\ &- c_{1i}\hat{z}_{1i}^2 + \hat{z}_{2i}\left[u_{b,i}(t) - u_i(t)\right] \\ &+ \frac{1}{\gamma_i}\tilde{\Theta}_i^T\dot{\tilde{\Theta}}_i + \frac{1}{\eta_i}\tilde{\varepsilon}_i^T\dot{\tilde{\varepsilon}}_i\end{aligned} \tag{50}$$

Using the Young's inequality $2a^T b \le \|a\|^2 + \|b\|^2$ we have

$$\begin{aligned}e_i^T P_i \delta_i &\le \frac{1}{2}\|e_i\|^2 + \frac{1}{2}\|P_i\|^2(\delta_{fi}^2 + \delta_{gi}^2) \\ &\le \frac{1}{2}\|e_i\|^2 + \frac{1}{2}\|P_i\|^2(\bar{\delta}_{fi}^2 + \bar{\delta}_{gi}^2)\end{aligned} \tag{51}$$

Substituting (51) into (50) results in

$$\begin{aligned}\dot{V} \le &\sum_{i=1}^{6} -e_i^T Q_i e_i + \frac{1}{2}\|e_i\|^2 \\ &+ \frac{1}{2}\|P_i\|^2(\bar{\delta}_{fi}^2 + \bar{\delta}_{gi}^2) \\ &- c_{1i}\hat{z}_{1i}^2 + \hat{z}_{2i}\left[u_{b,i}(t) - u_i(t)\right] \\ &+ \frac{1}{\gamma_i}\tilde{\Theta}_i^T\dot{\tilde{\Theta}}_i + \frac{1}{\eta_i}\tilde{\varepsilon}_i^T\dot{\tilde{\varepsilon}}_i\end{aligned} \tag{52}$$

Substituting (36) and (41) in (52), one have

$$\begin{aligned}\dot{V} = &\sum_{i=1}^{6} -e_i^T\left(Q_i - \frac{1}{2}I\right)e_i \\ &+ \frac{1}{2}\|P_i\|^2(\bar{\delta}_{fi}^2 + \bar{\delta}_{gi}^2) - c_{1i}\hat{z}_{1i}^2 \\ &+ \hat{z}_{2i}[\Theta_i^{*T}\varphi_i(\hat{X}) + \varepsilon_i - \Theta_i^T\varphi_i(\hat{X}) - u_{r,i} - c_{2i}\hat{z}_{2i}] \\ &+ \frac{1}{\gamma_i}\tilde{\Theta}_i^T\dot{\tilde{\Theta}}_i + \frac{1}{\eta_i}\tilde{\varepsilon}_i^T\dot{\tilde{\varepsilon}}_i\end{aligned} \tag{53}$$

The optimal parameters vector Θ_i^* and δ_i^* are slowly time varying, therefore the derivative of estimation error will be $\dot{\tilde{\Theta}}_i = -\dot{\Theta}_i$, and $\dot{\tilde{\varepsilon}}_i = -\dot{\hat{\varepsilon}}_i$. One have

$$\begin{aligned}\dot{V} = &\sum_{i=1}^{6} -e_i^T\left(Q_i - \frac{1}{2}I\right)e_i \\ &+ \frac{1}{2}\|P_i\|^2(\bar{\delta}_{fi}^2 + \bar{\delta}_{gi}^2) \\ &- c_{1i}\hat{z}_{1i}^2 - c_{2i}\hat{z}_{2i}^2 + \hat{z}_{2i}\tilde{\Theta}_i^T\varphi_i(\hat{X}) \\ &+ \hat{z}_{2i}[\varepsilon_i - u_{r,i}] - \frac{1}{\gamma_i}\tilde{\Theta}_i^T\dot{\Theta}_i - \frac{1}{\eta_i}\tilde{\varepsilon}_i^T\dot{\hat{\varepsilon}}_i\end{aligned} \tag{54}$$

$$\begin{aligned}\dot{V} \le &\sum_{i=1}^{6} -e_i^T\left(Q_i - \frac{1}{2}I\right)e_i \\ &+ \frac{1}{2}\|P_i\|^2(\bar{\delta}_{fi}^2 + \bar{\delta}_{gi}^2) \\ &- c_{1i}\hat{z}_{1i}^2 - c_{2i}\hat{z}_{2i}^2 + \frac{1}{\gamma_i}\tilde{\Theta}_i^T[\gamma_i\hat{z}_{2i}\varphi_i(\hat{X}) - \dot{\Theta}_i] \\ &+ \left|\hat{z}_{2i}\right|\varepsilon_i^* - \hat{z}_{2i}u_{r,i} + \frac{1}{\eta_i}\tilde{\varepsilon}_i[\eta_i\hat{z}_{2i}\tanh(\frac{\hat{z}_{2i}}{\epsilon_i}) - \dot{\hat{\varepsilon}}_i] \\ &- \varepsilon_i^*\hat{z}_{2i}\tanh(\frac{\hat{z}_{2i}}{\epsilon_i}) + \hat{\varepsilon}_i\hat{z}_{2i}\tanh(\frac{\hat{z}_{2i}}{\epsilon_i})\end{aligned} \tag{55}$$

Note that the following inquality hold for any $\zeta > 0$:

$$\left|\hat{z}_{2i}\right| - \hat{z}_{2i}\tanh(\frac{\hat{z}_{2i}}{\epsilon_i}) \le \zeta\epsilon_i = \varsigma \tag{56}$$

where ζ is a constant that satisfies $\zeta = e^{-(\zeta+1)}$, i.e. $\zeta = 0.2785$.
Substitute the parameter adaptive laws $\dot{\Theta}_i$ (43), the robust term $u_{r,i}$ (44) and $\dot{\hat{\varepsilon}}_i$ (45) into (55) and using (56), one obtains

$$\begin{aligned}\dot{V} \le &\sum_{i=1}^{6} -e_i^T\left(Q_i - \frac{1}{2}I\right)e_i \\ &+ \frac{1}{2}\|P_i\|^2(\bar{\delta}_{fi}^2 + \bar{\delta}_{gi}^2) \\ &- c_{1i}\hat{z}_{1i}^2 - c_{2i}\hat{z}_{2i}^2 + \varepsilon_i^*\varsigma \\ &+ \frac{\sigma_{1i}}{\gamma_i}\tilde{\Theta}_i^T\Theta_i + \frac{\sigma_{2i}}{\eta_i}\tilde{\varepsilon}_i\hat{\varepsilon}_i\end{aligned} \tag{57}$$

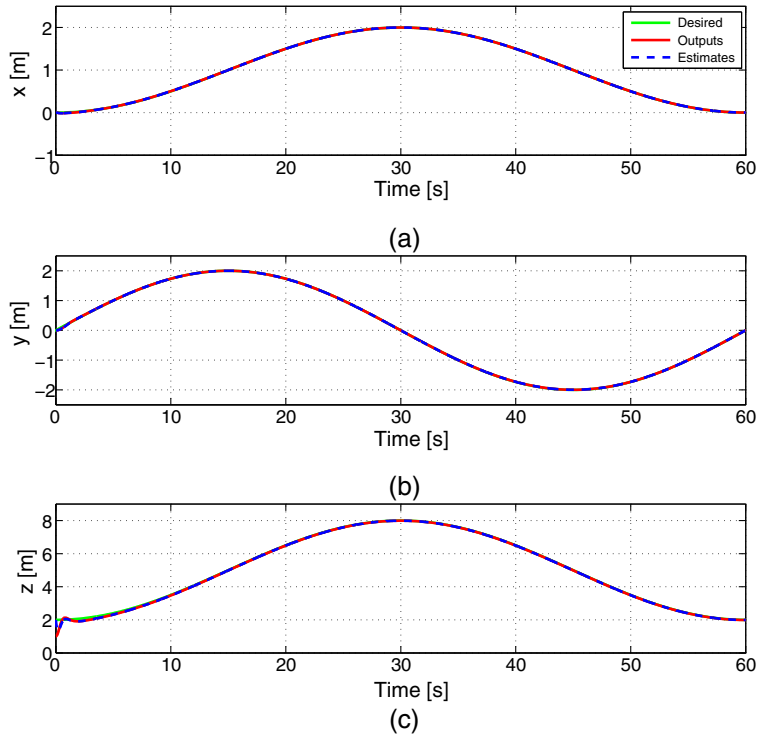

Fig. 5 Position tracking without external disturbances, scenario 1: (**a**) x position, (**b**) y position, (**c**) z position

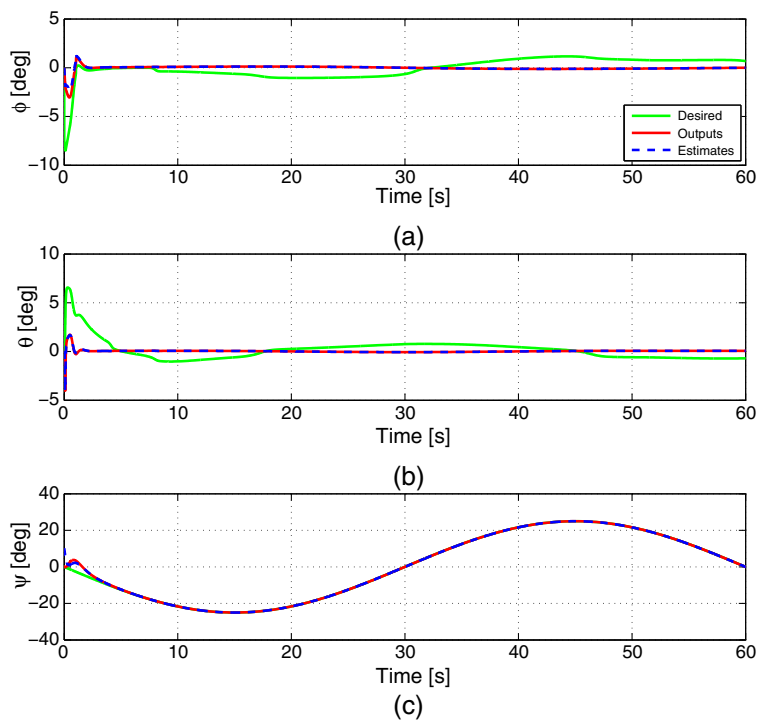

Fig. 6 Attitude tracking without external disturbances, scenario 1: (**a**) ϕ roll angle, (**b**) θ pitch angle, (**c**) ψ yaw angle

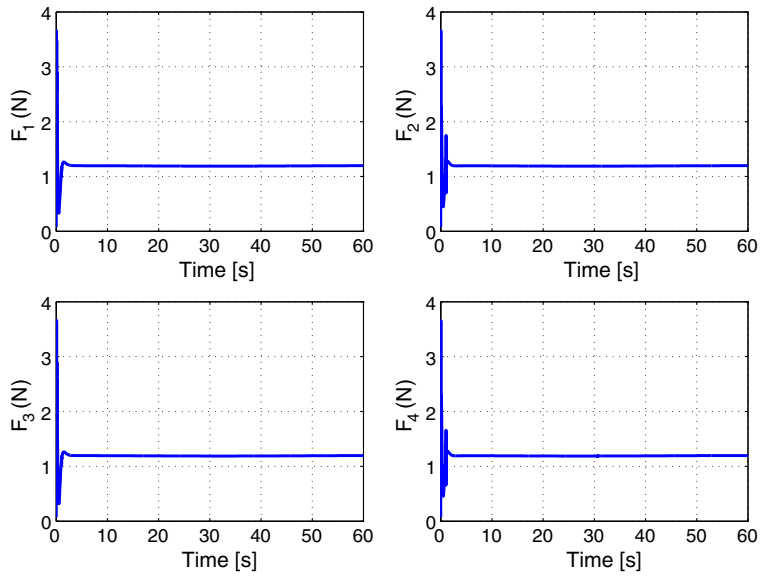

Fig. 7 Control inputs without external disturbances, scenario 1

Using Youngs' inequality for the term $\frac{\sigma_{1i}}{\gamma_i}\tilde{\Theta}_i^T\Theta_i$ and $\frac{\sigma_{2i}}{\eta_i}\tilde{\varepsilon}_i\hat{\varepsilon}_i$, one has the following inequalities:

$$\frac{\sigma_{1i}}{\gamma_i}\tilde{\Theta}_i^T\Theta_i \leq -\frac{\sigma_{1i}}{2\gamma_i}\tilde{\Theta}_i^T\tilde{\Theta}_i + \frac{\sigma_{1i}}{2\gamma_i}\Theta_i^{*T}\Theta_i^* \tag{58}$$

$$\frac{\sigma_{2i}}{\eta_i}\tilde{\varepsilon}_i\hat{\varepsilon}_i \leq -\frac{\sigma_{2i}}{2\eta_i}\tilde{\varepsilon}_i^2 + \frac{\sigma_{2i}}{2\eta_i}|\varepsilon_i^*|^2 \tag{59}$$

Therefore, (57) can be rewritten in the following form:

$$\begin{aligned}\dot{V} \leq & \sum_{i=1}^{6} -e_i^T\left(Q_i - \frac{1}{2}I\right)e_i - c_{1i}\hat{z}_{1i}^2 - c_{2i}\hat{z}_{2i}^2 \\ & - \frac{\sigma_{1i}}{2\gamma_i}\tilde{\Theta}_i^T\tilde{\Theta}_i + \frac{\sigma_{1i}}{2\gamma_i}\Theta_i^{*T}\Theta_i^* + \frac{1}{2}\|P_i\|^2\bar{\delta}_{fi}^2 \\ & - \frac{\sigma_{2i}}{2\eta_i}\tilde{\varepsilon}_i^2 + \frac{\sigma_{2i}}{2\eta_i}|\varepsilon_i^*|^2 + \varepsilon_i^*\varsigma + \frac{1}{2}\|P_i\|^2\bar{\delta}_{gi}^2\end{aligned} \tag{60}$$

Define $c = \min\{2\min(\lambda_{\min}(Q_i) - 1/2), \sigma_{1i}, \sigma_{2i}, 2c_{1i}, 2c_{2i}\}$, then (60) becomes

$$\dot{V} \leq -cV + \rho \tag{61}$$

where

$$\begin{aligned}\rho = & \sum_{i=1}^{6}\frac{\sigma_{1i}}{2\gamma_i}\Theta_i^{*T}\Theta_i^* + \frac{\sigma_{2i}}{2\eta_i}|\varepsilon_i^*|^2 \\ & + \frac{1}{2}\|P_i\|^2(\bar{\delta}_{fi}^2 + \bar{\delta}_{gi}^2) + \varepsilon_i^*\varsigma\end{aligned}$$

Now we can prove the following theorem that shows our main result in this paper.

Theorem 1 *Consider the quadrotor nonlinear system (19). Suppose the assumptions 1-5 and lemma 1 hold. Then the observer-based adaptive fuzzy control law described by (42) with parameter adaptation law given by (43) and (45) guarantees that all the signals of the closed-loop system are UUB stable and the output tracking error converges to a small neighborhood of the origin. Furthermore, the designed controller can ensure robustness against wind gust disturbance.*

Proof Integrating (61) over $[0, t]$, obtain

$$V(t) \leq V(0)e^{-ct} + \frac{\rho}{c} \tag{62}$$

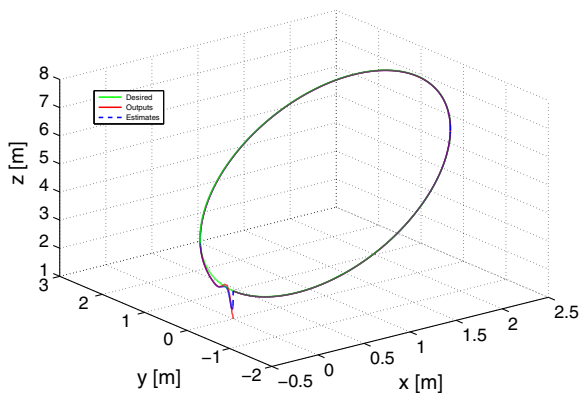

Fig. 8 3D-Position without external disturbances, scenario 1

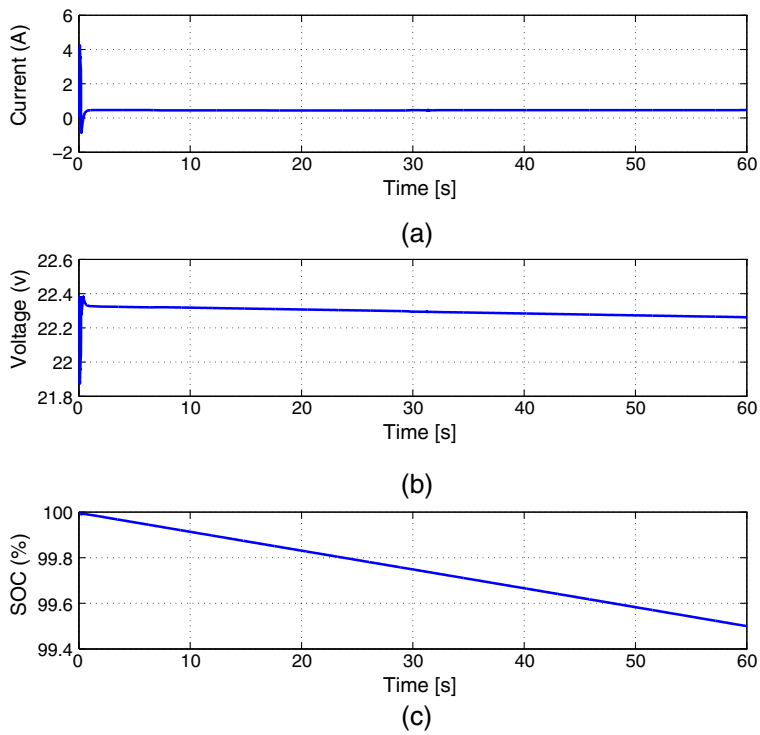

Fig. 9 Discharge experiment, scenario 1: (**a**) I_{bat} battery current, (**b**) V_{bat} battery voltage, SOC state of charge

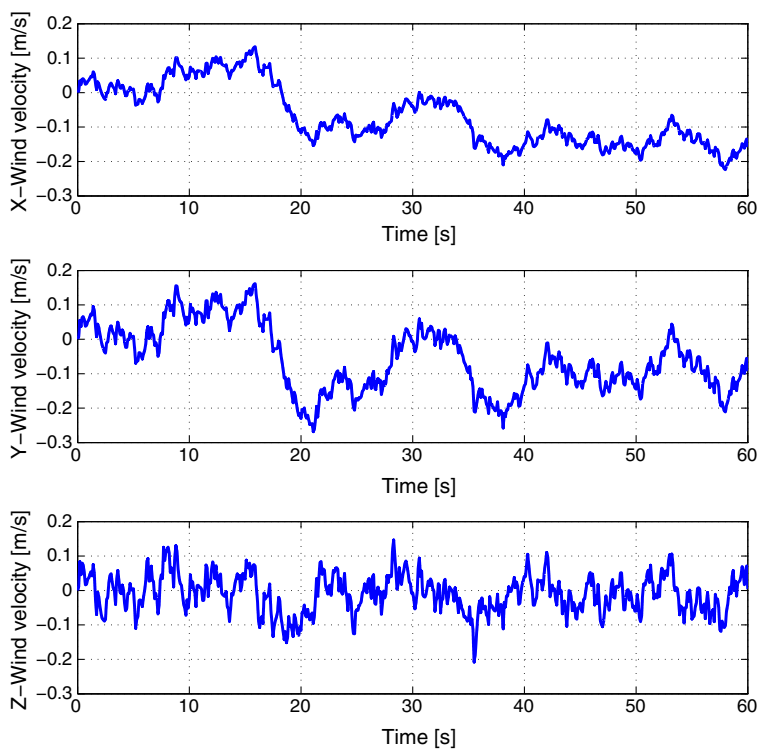

Fig. 10 Wind velocity

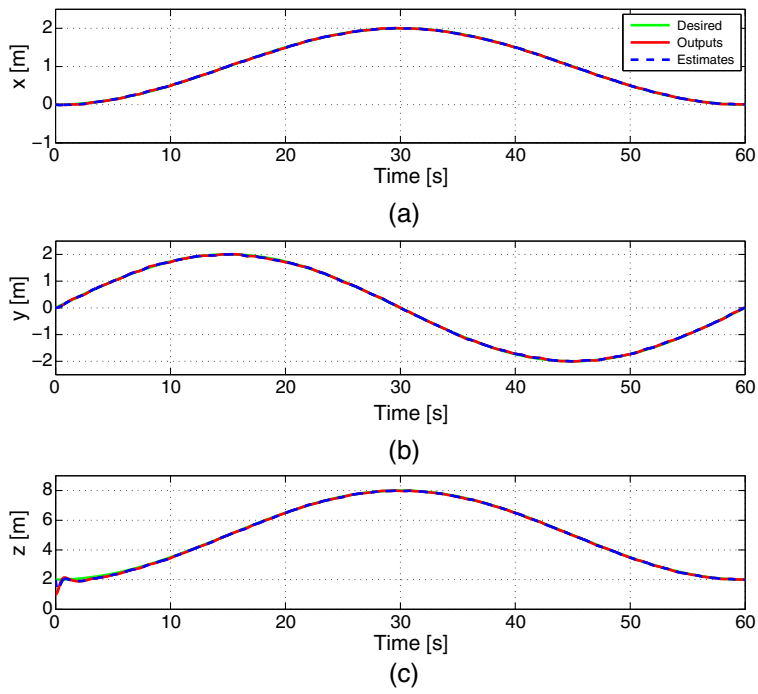

Fig. 11 Position tracking with external disturbances, scenario 2: (**a**) x position, (**b**) y position, (**c**) z position

The inequality (61), implies that for $V \geq \rho/c$, $\dot{V} \leq 0$. Therefore, using Lyapunov theorem, the signals $\hat{z}_{1i}(t)$, $\hat{z}_{2i}(t)$, $e_i(t)$, $\tilde{\Theta}_i(t)$, $\tilde{\varepsilon}_i$ and $u(t)$ in the the closed-loop system are bounded, as well as the system states x_{1i}, x_{2i}, $\hat{x}_{1i}$ and $\hat{x}_{2i}$; moreover, for any $\mu \geq \sqrt{\rho/c}$, there exists a constant $T > 0$, such that $\left|\hat{z}_{1i}(t)\right| \leq \mu$ for all $t \geq T$. In order to achieve the tracking error convergence to a small neighborhood

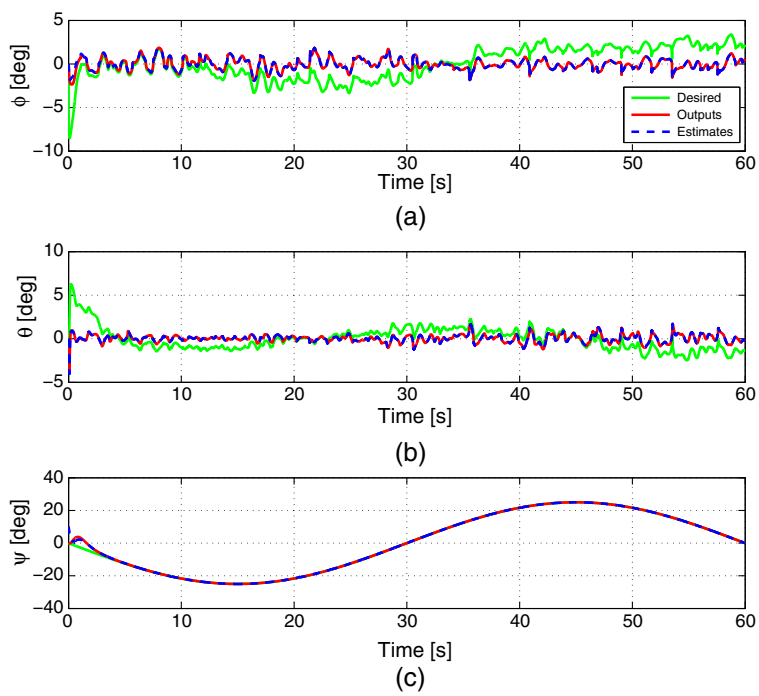

Fig. 12 Attitude tracking with external disturbances, scenario 2: (**a**) ϕ roll angle, (**b**) θ pitch angle, (**c**) ψ yaw angle

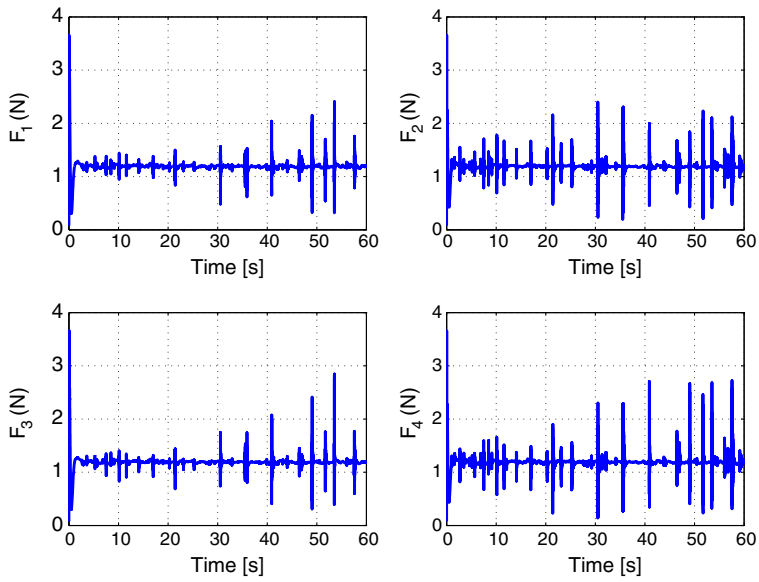

Fig. 13 Control inputs with external disturbances, scenario 2

around zero and make $\sqrt{\rho/c}$ as small as desired, the design parameters $\gamma_i, \eta_i, \epsilon_i, \sigma_{1i}, \sigma_{2i}, c_{1i}$ and c_{2i} should be chosen appropriately. Thus, it is easy to see that $\lim_{t\to\infty} \left|\hat{z}_{1i}(t)\right| \leq \mu$. This completes the proof. □

Remark 3 In the adaptive laws (43) and (45), σ-modification term was used to avoid parameters drift caused by the approximation errors. We notice that the adaptive laws are modified so that the time derivative of the Lyapunov function used to analyze these adaptive laws becomes negative in the space of the parameter estimates when these parameters exceed certain bounds [54].

5 Simulation Results

In order to validate the designed AFBC strategy, simulations are made to check the robustness and performances attained by proposed controller for the trajectory tracking problem. Three simulation scenarios are made. In the first scenario a circular trajectory is considered without taking into account external disturbances and parametric uncertainties. In the second scenario, external disturbances (wind gust) are considered. In the third scenario, a spiral trajectory is considered with parametric uncertainties (in the elements of inertia matrix).

The wind gust model presented in Section 2.3 is used to generate wind velocity along the three axis (lateral, longitudinal and vertical). Then they are considered as additive external disturbances to the translational velocity of the QUAV. Parameters of the wind gust model are: $L_u = L_v = 23.568$, $L_w = 3$, $\sigma_u = \sigma_v = 0.68$, $\sigma_w = 0.34$, and a typical wind speed of $3.4m/s$ is considered. A variation of 40 % for inertia parameters (I_x, I_y, I_z) is considered to test the robustness provided by the proposed control strategy with respect to parametric uncertainties.

The quadrotor parameters model used in simulation are: $m = 0.486kg$, $l = 0.25m$, $I_x = I_y = 0.0038kgm^2$, $I_z = 0.0076kgm^2$, $I_r = 3.35710^{-5}kgm^2$, $b = 2.98410^{-5}$, $d = 3.23210^{-7}$ and $g = 9.81m/s^2$. Where the design parameters are chosen as $c_{11} = 0.3, c_{12} = 0.4, c_{13} = 1, c_{14} = 3, c_{15} =$

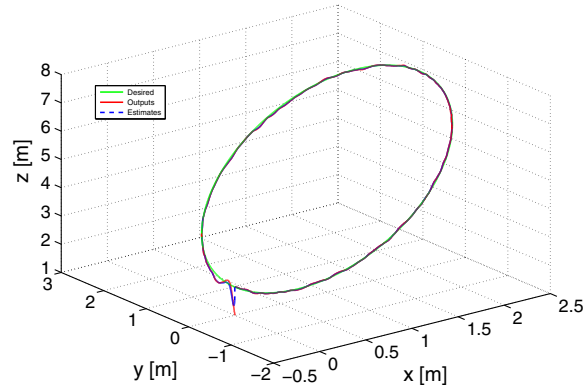

Fig. 14 3D-Position with external disturbances, scenario 2

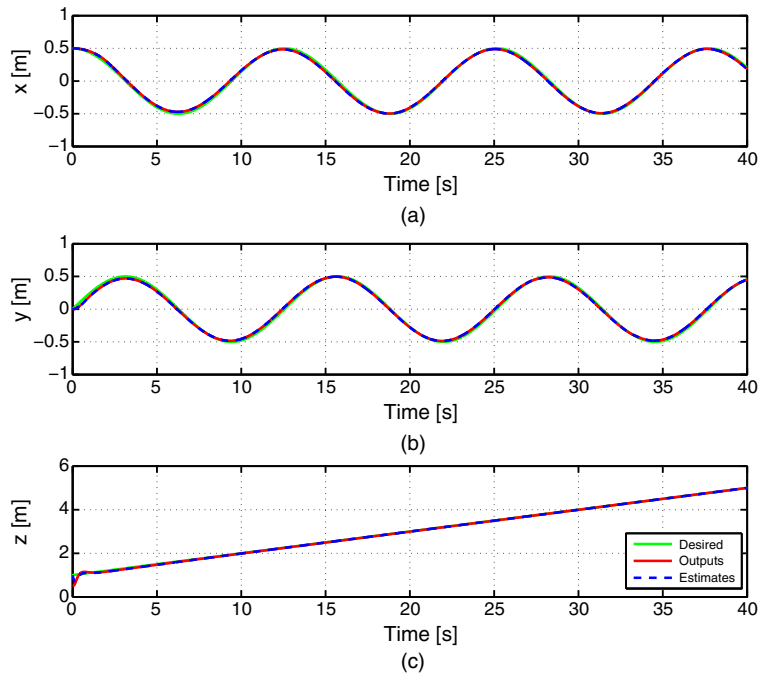

Fig. 15 Position tracking with parametric uncertainties, scenario 3: (**a**) x position, (**b**) y position, (**c**) z position

$5, c_{16} = 3, k_{11} = 8, k_{12} = 8, k_{13} = 5, k_{14} = 8, k_{15} = 8, k_{16} = 8, c_{21} = 0.6, c_{22} = 0.8, c_{23} = 2, c_{24} = 6, c_{25} = 10, c_{26} = 6, k_{21} = 16, k_{22} = 16, k_{23} = 10, k_{24} = 16, k_{25} = 16, k_{26} = 16$. The gains of the fuzzy adaptive laws are chosen as $\gamma_i = 0.9(i = 1, 2, 3, 5, 6), \gamma_4 = 1.8, \sigma_{1i} = 0.01$ and the robust control gains $\epsilon_i = 0.001, \eta_i = 0.03$ and $\sigma_{2i} = 0.01$. The sampling time is given by $\Delta t = 0.001s$.

The initial positions and Euler angles are chosen as $x_{11}(0) = 0, x_{12}(0) = 0, x_{13}(0) = 0, x_{14}(0) =$

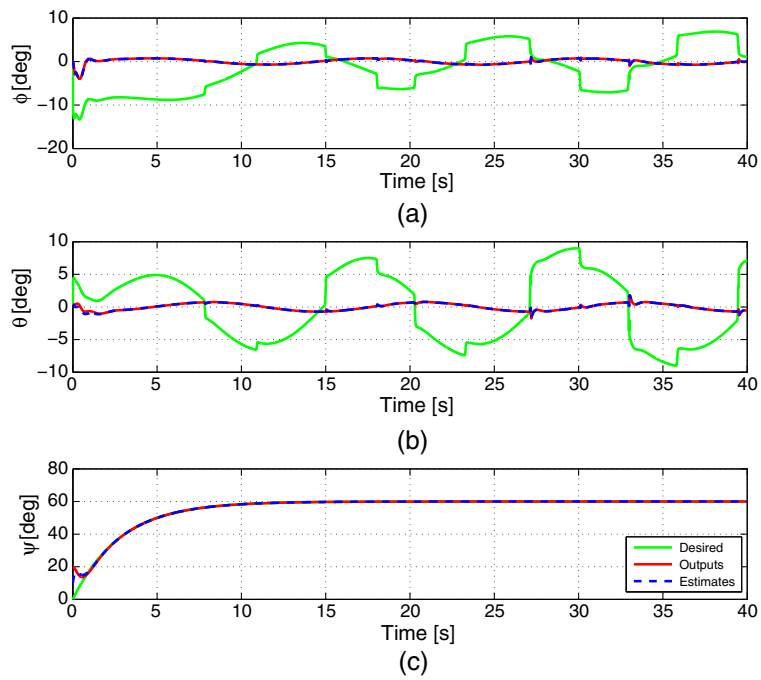

Fig. 16 Attitude tracking with parametric uncertainties, scenario 3: (**a**) ϕ roll angle, (**b**) θ pitch angle, (**c**) ψ yaw angle

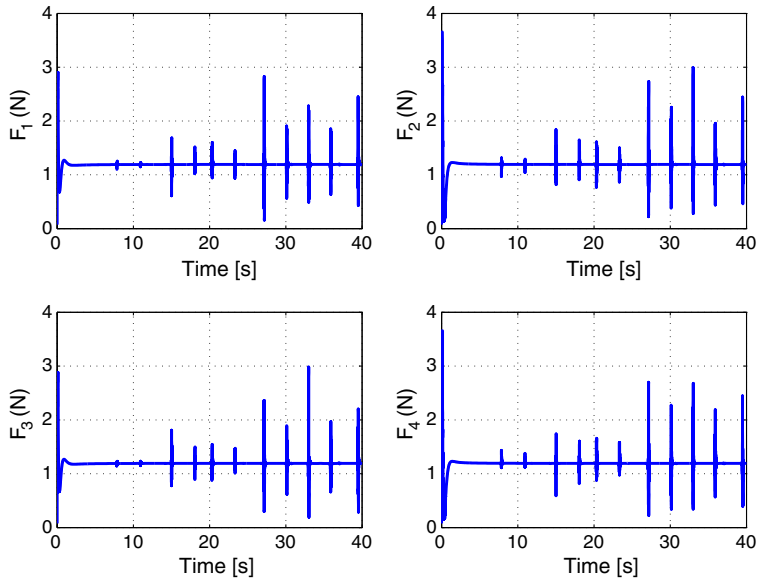

Fig. 17 Control inputs with parametric uncertainties, scenario 3

$1, x_{15}(0) = 0, x_{16}(0) = 0, \hat{x}_{11}(0) = 0, x_{12}(0) = 0, \hat{x}_{13}(0) = 0.179, \hat{x}_{14}(0) = 2, \hat{x}_{15}(0) = 0, \hat{x}_{16}(0) = 0$, and initial values of adaptive laws $\hat{\varepsilon}_i(0) = 0$, $\Theta_i(0) = [0, 0, 0, 0, 0, 0, 0, 0, 0]$. The initial linear and angular velocities are chosen equal to zero. The input variables of the FLS (42) are chosen as $x_{Fi} = [x_{1i}, \dot{x}_{1i}]^T$ for angles system ($i = 1, 2, 3$), and $z_{Fi} = [z_{1i}, \dot{z}_{1i}]^T$ for position system ($i = 4, 5, 6$). For each variable x_{Fi} and z_{Fi}, three Gaussian membership functions are defined as

$$\mu_{F^1_{x_i}} = \exp\left(-\frac{1}{2}\left(\frac{x_{Fi}+0.26}{0.1}\right)^2\right), \mu_{F^1_{z_i}} = \exp\left(-\frac{1}{2}\left(\frac{z_{Fi}+10}{4}\right)^2\right)$$

$$\mu_{F^2_{x_i}} = \exp\left(-\frac{1}{2}\left(\frac{x_{Fi}}{0.1}\right)^2\right), \mu_{F^2_{z_i}} = \exp\left(-\frac{1}{2}\left(\frac{z_{Fi}}{4}\right)^2\right)$$

$$\mu_{F^3_{x_i}} = \exp\left(-\frac{1}{2}\left(\frac{x_{Fi}-026}{0.1}\right)^2\right), \mu_{F^3_{z_i}} = \exp\left(-\frac{1}{2}\left(\frac{z_{Fi}-10}{4}\right)^2\right)$$

Scenario 1: Circular trajectory without external disturbances and parametric uncertainties

The first desired trajectory used is a circle of 8 meter high evolving in the Cartesian space defined by

$$x_d = 1 - \sin(\frac{\pi t}{30} + \frac{\pi}{2})m, y_d = -2\sin(\frac{\pi t}{30} + \pi)m$$

$$z_d = 5 - 3\sin(\frac{\pi t}{30} + \frac{\pi}{2})m, \psi_d = 0.43\sin(\frac{\pi t}{30} + \pi)rad$$

Simulation results for trajectory tracking of this desired trajectory are presented in Figs. 5, 6, 7, and 8. The 3D desired trajectory and the corresponding AFBC quadrotor trajectory are illustrated in Fig. 8, while the tracking responses of the QUAV position and attitude are presented in Figs. 5 and 6 respectively. It can be observed that the tracking is achieved with null error in all quadrotor outputs for the AFBC scheme. Figure 6 shows how the desired roll and pitch angles change their values in an interval of $20deg$ between -10 and $+10deg$ to ensure an appropriate tracking performance for x and y motion. As depicted in Fig. 7, the AFBC strategy generates smooth input control signals.

Figure 9, represent battery discharge experiment. From battery state of charge SOC we can have an idea about the power consumed by the QUAV and the

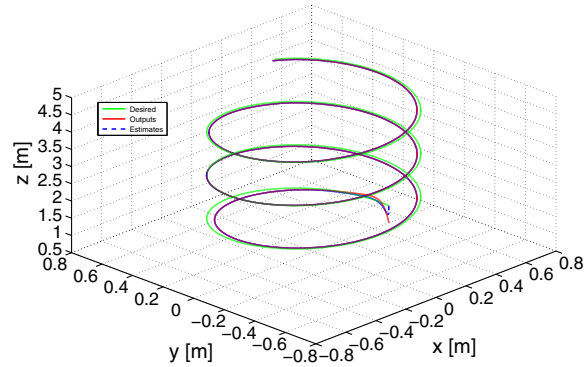

Fig. 18 3D-Position with parametric uncertainties, scenario 3

flight time, then we can describe the effect of battery discharge on the flight performance.

Scenario 2: Circular trajectory with external disturbances

Simulation results for this scenario are presented in Figs. 10, 11, 12, 13 and 14. The computed wind velocities applied on the translational velocity of the QUAV are shown in Fig. 10. It can be clearly seen how starting from an initial position far from the desired position, the proposed AFBC strategy is capable to make the quadrotor track the desired trajectory despite the presence of external disturbances (wind gust effect). In addition, Figs. 11–12 show the good tracking performances for quadrotor outputs given by the proposed controller. We can see clearly the effect of wind gust on the quadrotor movement in roll and pitch angles (Fig. 11), position in 3D space (Fig. 14) and control inputs (Fig. 13). It is noted that the control inputs change their values to ensure the control task.

Scenario 3: Spiral trajectory with parametric uncertainties

The third simulation study has been carried out with a spiral desired trajectory of 5 meter high, given by:

$$x_d = \frac{1}{2}\sin(\frac{t}{2})m,\ y_d = \frac{1}{2}\sin(\frac{t}{2})m$$
$$z_d = 1 + \frac{t}{10}m,\ \psi_d = \frac{\pi}{3}rad$$

Figures 15, 16, 17, 18 show quadrotor outputs and control inputs for this scenario. The control task is achieved with good tracking performances, and robustness against parametric uncertainties is improved by the proposed controller.

6 Conclusion

In this work, we have presented a robust AFBC scheme based on state observer for QUAV, in the presence of wind gust disturbances and parametric uncertainties. The Lyapunov function was used to develop the algorithm and the parameter adaptive law. The design can be used to attenuate the effect of aerodynamic disturbances and parametric uncertainties acting on the QUAV, while keeping tracking control efficiency and bounded stability of the global closed-loop system. Unlike active disturbances rejection design, the proposed algorithm does not require a priori knowledge about external disturbances and dynamic model. Therefore, the proposed controller can operate in harsh environment conditions such as wind gust associated with model uncertainties and nonlinear aerodynamic friction. Simulation results show good tracking performances for different classes of trajectories, and illustrate the robust performance provided by the AFBC scheme.

References

1. Raffo, G.V., Ortega, M.G., Rubio, F.R.: Asian J. Control **17**(1), 142 (2015)
2. Raffo, G.V., Ortega, M.G., Rubio, F.R.: Automatica **46**(1), 29 (2010)
3. Dydek, Z., Annaswamy, A., Lavretsky, E.: IEEE Trans. Control Syst. Technol. **21**(4), 1400 (2013)
4. Tayebi, A., McGilvray, S.: In: 43rd IEEE Conference on Decision and Control (CDC), vol. 2, pp. 1216–1221 (2004)
5. Castillo, P., Lozano, R., Dzul, A.: In: IEEE/RSJ International Conference on Intelligent Robots and Systems (IROS), vol. 3, pp. 2693–2698 (2004)
6. Bouabdallah, S., Noth, A., Siegwart, R.: In: IEEE/RSJ International Conference on Intelligent Robots and Systems (IROS), vol. 3, pp. 2451–2456 (2004)
7. Mian, A.A., Daobo, W.: Chin. J. Aeronaut. **21**(3), 261 (2008)
8. Basri, M.A.M., Husain, A.R., Danapalasingam, K.A.: J. Intell. Robot. Syst. **79**(2), 295 (2015)
9. Lee, D., Kim, H.J., Sastry, S.: Int. J. Control Autom. Syst. **7**(3), 419 (2009)
10. Besnarda, L., Shtesselb, Y.B., Landrum, B.: J. Franklin Inst. **349**(2), 658 (2012)
11. Zuo, Z.: Control Theory Appl. IET **4**(11), 2343 (2010)
12. Castillo, P., Dzul, A., Lozano, R.: IEEE Trans. Control Syst. Technol. **12**(4), 510 (2004)
13. Cao, N., Lynch, A.: IEEE Trans. Control Syst. Technol. (2016). doi:10.1109/TCST.2015.2505642
14. Chen, H., Wang, C., Yang, L., Zhang, D.: J. Dyn. Syst. Measur. Control **134**(4), 61 (2012)
15. Chen, H., Wang, C., Zhang, B., Zhang, D.: Trans. Inst. Meas. Control. **35**(2), 105 (2013)
16. Chen, H.: Int. J. Control Autom. Syst. **12**(6), 1216 (2014)
17. Kendoul, F., Lara, D., Fantoni, I., Lozano, R.: In: 45th IEEE Conference on Decision and Control (CDC), pp. 5888–5893 (2006)
18. Madani, T., Benallegue, A.: In: American Control Conference (ACC), pp. 5887–5892 (2007)
19. Pollini, L., Metrangolo, A.: In: AIAA Modeling and Simulation Technologies Conference (2008)
20. Escareño, J., Salazar, S., Romero, H., Lozano, R.: J. Intell. Robot. Syst. **70**(1–4), 51 (2013)
21. Ramirez-Rodriguez, H., Parra-Vega, V., Sanchez-Orta, A., Garcia-salazar, O.: J. Intell. Robot. Syst. **73**(1–4), 51 (2014)
22. Huang, M., Xian, B., Diao, C., Yang, K., Feng, Y.: In: American Control Conference (ACC), pp. 2076–2081 (2010)

23. Lee, D., Nataraj, C., Burg, T.C., Dawson, D.M.: In: American Control Conference (ACC), pp. 2326–2331 (2011)
24. Alexis, K., Nikolakopoulos, G., Tzes, A.: Asian J. Control **16**(1), 209 (2014)
25. Basri, M.A.M., Husain, A.R., Danapalasingam, K.A.: Trans. Inst. Measur. Control **37**(3), 345 (2015)
26. Das, A., Lewis, F., Subbarao, K.: J. Intell. Robot. Syst. **56**(1–2), 127 (2009)
27. Boudjedir, H., Bouhali, O., Rizoug, N.: Adv. Robot. **28**(17), 1151 (2014)
28. Wang, L.X.: Adaptive Fuzzy Systems and Control: Design and Stability Analysis. Prentice-Hall, Inc., NJ, USA (1994)
29. Tong, S.C., Li, Y.M., Feng, G., Li, T.S.: IEEE Trans. Syst. Man Cybern. Part B: Cybern. **41**(4), 1124 (2011)
30. Lee, H.: IEEE Trans. Fuzzy Syst. **19**(2), 265 (2011)
31. Zhou, Q., Shi, P., Lu, J., Xu, S.: IEEE Trans. Fuzzy Syst. **19**(5), 972 (2011)
32. Chwa, D.: IEEE Trans. Fuzzy Syst. **20**(3), 587 (2012)
33. Chen, B., Liu, X.P., Ge, S.S., Lin, C.: IEEE Trans. Fuzzy Syst. **20**(6), 1012 (2012)
34. Tong, S., Li, Y.: IEEE Trans. Fuzzy Syst. **20**(1), 168 (2012)
35. Liu, Z., Wang, F., Zhang, Y., Chen, X., Chen, C.P.: IEEE Trans. Cybern. **44**(10), 1714 (2014)
36. Zhou, Q., Shi, P., Xu, S., Li, H.: IEEE Trans. Fuzzy Syst. **21**(2), 301 (2013)
37. Wang, T., Zhang, Y., Qiu, J., Gao, H.: IEEE Trans. Fuzzy Syst. **23**(2), 302 (2015)
38. Li, Y., Tong, S., Liu, Y., Li, T.: IEEE Trans. Fuzzy Syst. **22**(1), 164 (2014)
39. Yu, J., Chen, B., Yu, H.: Nonlinear Dyn. **69**(3), 1479 (2012)
40. Li, Y., Tong, S., Li, T.: Nonlinear Dyn. **73**(1–2), 133 (2013)
41. Li, Y., Tong, S., Li, T.: Neural Comput. Appl. **23**(5), 1207 (2013)
42. Yacef, F., Bouhali, O., Hamerlain, M.: In: IEEE International Conference on Unmanned Aircraft Systems (ICUAS), pp. 920–927 (2014)
43. Garcia, P.C., Lozano, R., Dzul, A.E.: Modelling and control of mini-flying machines. Springer Science & Business Media (2006)
44. Escareño, J., Salazar-Cruz, S., Lozano, R.: In: American Control Conference (ACC), pp. 3936–3941 (2006)
45. Hoffmann, G.M., Huang, H., Waslander, S.L., Tomlin, C.J.: In: AIAA Guidance, Navigation and Control Conference, vol. 2 (2007)
46. Pounds, P., Mahony, R., Corke, P.: In: Proceedings Australasian Conference on Robotics and Automation 2006 (2006)
47. Podhradskỳ, M., Coopmans, C., Jensen, A.: J. Intell. Robot. Syst. **74**(1–2), 193 (2014)
48. Mesbahi, T., Rizoug, N., Bartholomeus, P., Le Moigne, P.: In: Vehicle Power and Propulsion Conference (VPPC), pp. 1–8. IEEE (2013)
49. Mollov, L., Kralev, J., Slavov, T., Petkov, P.: J. Intell. Robot. Syst. **76**(2), 315 (2014)
50. Etele, J.: Overview of Wind Gust Modelling with Application to Autonomous Low-Level UAV Control. Defence Research and Development Canada (2006)
51. Alexis, K., Nikolakopoulos, G., Tzes, A.: In: MELECON 15th IEEE Mediterranean Electrotechnical Conference, pp. 1411–1416 (2010)
52. Ahmed, B., Kendoul, F.: In: 49th IEEE Conference on Decision and Control (CDC), pp. 3536–3541 (2010)
53. Slotine, J.J., Li, W., et al.: Applied Nonlinear Control, vol. 199. Prentice Hall Englewood Cliffs, NJ (1991)
54. Ioannou, P., Sun, J.: Robust Adaptive Control. Prentice Hall, Inc (1996)

Fouad Yacef is a researcher at the Centre de Dévelopment des Technologies Avancées (CDTA). He received his Magister degree in Automatic Control from the Ecole Militaire Polytechnique (EMP), Algeria in 2009. He is currently a PhD student at Jijel University, Algeria and the Ecole Supérieure des Techniques Aéronautiques et de Construction Automobile (ESTACA), France. His research interests include Adaptive control, Fuzzy control, energy management systems and their applications in unmanned aerial vehicles.

Omar Bouhali is a professor and the Director of MecaTronic Laboratory (LMT), Jijel University. He received the PhD degree from the Central School of Lille, France and National Polytechnic School of Algeria in 2007. His research focuses on adaptive non-linear control using universal approximates and renewable energy-based power systems with storage using multilevel converters.

Mustapha Hamerlain is a research director at the Centre de Dévelopment des Technologies Avancées (CDTA). He received the PhD degree from the Institut National des Sciences Appliquées de Toulouse (INSA), France in 1993. His research focuses on sliding mode control, adaptive control and nonlinear robotic system.

Nassim Rizoug received the PhD in Electrical Engineering from the Ecole Centrale de Lille, France, in 2006. He is currently an assistant professor at the Ecole Supérieure des Techniques Aéronautiques et de Construction Automobile (ESTACA), France since 2007. His research interest includes specially the field of energy management, the characterization of the storage component for the power electronic applications and systems control.